PHYSICAL REVIEW A VOLUME 46, NUMBER 7 1 OCTOBER 1992

Collisional deactivation for K in high-lying ${}^2S$ and ${}^2D$ states by H_2

Yeung-Long Luo, King-Chuen Lin,* Dean-Kuo Liu, and Hui-Jean Liu
Department of Chemistry, National Taiwan University, Taipei, Taiwan, Republic of China
and Institute of Atomic and Moleclar Sciences, Academia Sinica, P.O. Box 23-166,
Taipei 10764, Taiwan, Republic of China

Wei-Tzou Luh
Institute of Atomic and Molecular Sciences, Academia Sinica, P.O. Box 23-166,
Taipei 10764, Taiwan, Republic of China

(Received 9 March 1992)

By using a kinetic model, we can easily resolve the observed effective lifetimes of the K $n\,{}^2S$ ($n=8$–11) and $n\,{}^2D$ ($n=6$–8) states in the presence of the H_2 gas. Thereby, in accordance with the Stern-Volmer equation, the radiative lifetimes and the collisional deactivation cross sections of these states can be determined. The lifetimes observed in this work agree satisfactorily with results reported elsewhere. The cross section for the $n\,{}^2S$ state increases with increasing n, whereas that for the $n\,{}^2D$ state tends to decrease. A qualitative explanation for this n dependence is given.

PACS number(s): 32.70.Fw

I. INTRODUCTION

In recent years, studies of mechanisms on energy depletion, population redistribution, and chemical reaction associated with the collisions of the alkali-metal atoms in moderately high-lying states with molecular perturbers have received much attention [1–6]. For instance, the intermultiplet transfers of Na($4D$) or Na($4P$) by H_2, N_2, and O_2 [1–3] as well as the quenching cross section of Rb($7S$-$5D$) transition by H_2, D_2, and He have been recently investigated [4]. The results are consistent with the theoretical prediction by means of the impulse approximation or multiple curve crossing model [1–4]. Using a crossed-beam apparatus to investigate the reaction of Cs($7P$) and H_2, Vetter and co-workers demonstrated that CsH may be produced in single collision [5,6]. The total cross sections for deactivation by noble gases, N_2, CO, and CH_4 of sodium atoms in various high-lying states have been found apparently to increase with increasing energy of the excited state of Na [7–10].

In previous work, we have first found that a single collision between the excited K atom and H_2 led to the formation of KH, via a state-selective reaction with K($7\,{}^2S$) [11]. No product was observed from collision with K($5\,{}^2D$). Such a large discrepancy in the relative chemical reactivity has been interpreted in terms of a harpoon mechanism with the symmetry correlation taken into account. Subsequently, the study on the physical quenching of these two states, which are radiatively metastable with respect to the ground state, has also been carried out. The total cross sections for deactivation of excited potassium atoms by collision with H_2 are (150 ± 2) Å^2 for the $7\,{}^2S$ state and (39 ± 4) Å^2 for the $5\,{}^2D$ state [12]. The cross section for the $7\,{}^2S$-$5\,{}^2D$ transition induced by collision has been measured; this transfer has also been proved to be the predominant channel for the depopulation of the $7\,{}^2S$ state [12].

In this work, we extend the studies on deactivation processes of the excited K atom by H_2 to its moderately high-lying states. The K $n\,{}^2S$ ($n=8-11$) or $n\,{}^2D$ ($n=6-8$) states are populated by a two-photon excitation. Compared to the low-lying states, these highly excited atoms may possess quite different effective size, polarizability, and reactivity [13]. Here we present our measurement on the radiative lifetimes and the total deactivation cross sections of these metastable states.

II. EXPERIMENT

The apparatus used to measure the time-resolved fluorescence of the excited K atoms has been illustrated in our previous work [14,15]. Only a brief description is given below.

The reaction chamber was a stainless-steel five-armed-cross heat-pipe oven, allowing for spectral observation perpendicular to the laser axis. A thermocouple, inserted through the top arm in the vicinity of the interactive region, was used to monitor the oven temperature with an accuracy ±1 K. The potassium metal was deposited and heated to a temperature of 470 K, corresponding to vapor pressure of 6 mTorr.

The radiation source was a tunable dye laser pumped by an Nd:YAG laser with a pulse duration 5–8 ns and repetition rate 10 Hz. The laser power was monitored simultaneously by an energy meter and was adjusted in the range 1–3 mJ. The K $n\,{}^2S$ or $n\,{}^2D$ states were populated by a two-photon absorption process, which was carefully confirmed by the quadratic laser-power dependence of their respective atomic fluorescence intensities. The time-resolved fluorescence on the $n\,{}^2S$ (or $n\,{}^2D$)-$4\,{}^2P$ transition was measured as a function of H_2 pressure in the range 20–300 mTorr, which was monitored with an MKS Baratron manometer. The obtained temporal profile was processed and averaged over 500 shots by a transient digitizer. It was found that the effective lifetimes for these high-lying states were much larger than the laser-pulse duration. Thus the laser profile could be considered as a δ function, and the detected temporal profile then corresponded to the population evolution of the excited state.

III. KINETIC MODELING

The K atoms in the $n\,^2S$ (or $n\,^2D$) states can relax by the processes of either radiative cascade or collisional deactivation. For simplicity, a three-level system is assumed. The depopulation process for the case of the $n\,^2S$ state is described as follows and depicted in Fig. 1:

$$A_2 \xrightarrow{k_1} A_1 + h\nu_1 \;, \tag{1}$$

$$A_2 + \mathrm{H}_2 \xrightarrow{k_2} A_1 + \mathrm{H}_2 \;, \tag{2}$$

$$A_2 + \mathrm{H}_2 \underset{k_{-3}}{\overset{k_3}{\rightleftarrows}} A_3 + \mathrm{H}_2 \;, \tag{3}$$

$$A_3 \xrightarrow{k_4} A_1 + h\nu_2 \;, \tag{4}$$

$$A_3 + \mathrm{H}_2 \xrightarrow{k_5} A_1 + \mathrm{H}_2 \;, \tag{5}$$

where k_i's, $i=1-5$ and -3, denote the first-order or second-order rate coefficients associated with the reaction scheme. A_2 represents the K($n\,^2S$) state, which is initially excited by a two-photon absorption. A_3 corresponds to the K[$(n-2)\,^2D$] state, closest to A_2. Since A_2 is just of slightly more energy than A_3, the repopulation process from A_3, as indicated in Eq. (3), cannot be neglected. A_1 assembles the remaining lower states. The solution to the relevant coupled-rate equations yields [12]

$$[A_2(t)] = [A_2]_0 (s_1 e^{-\lambda_1 t} + s_2 e^{-\lambda_2 t}) \;. \tag{6}$$

Here

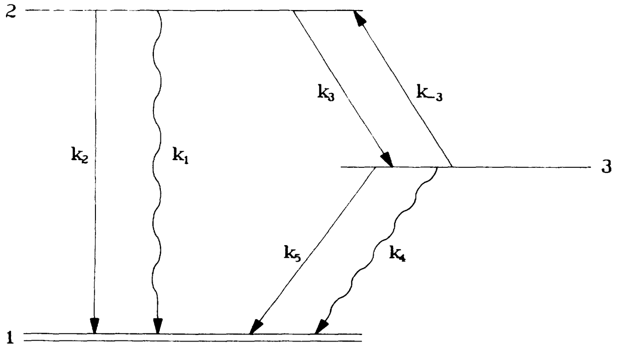

FIG. 1. Energy diagram of a three-level system. k_1 and k_4 indicate the rate coefficients for radiative cascade; k_2, k_3, and k_5 indicate the rate coefficients for collisional deactivation; k_{-3} is the rate coefficient for collisional activation.

$$s_1 = \frac{\lambda_2 - C_{11}}{\lambda_2 - \lambda_1} \;, \tag{7}$$

$$s_2 = \frac{C_{11} - \lambda_1}{\lambda_2 - \lambda_1} \;, \tag{8}$$

$$C_{11} = (k_2 + k_3)[\mathrm{H}_2] + k_1 \;, \tag{9}$$

$$C_{12} = k_{-3}[\mathrm{H}_2] \;, \tag{10}$$

$$C_{21} = k_3[\mathrm{H}_2] \;, \tag{11}$$

$$C_{22} = (k_{-3} + k_5)[\mathrm{H}_2] + k_4 \;, \tag{12}$$

and

$$\lambda_{1,2} = \tfrac{1}{2}\{ (C_{11}+C_{22}) \pm [(C_{11}+C_{22})^2 - 4(C_{11}C_{22} - C_{12}C_{21})]^{1/2} \} \;. \tag{13}$$

λ_1 and λ_2 represent the plus and minus signs, respectively. The population of the excited state is assumed to be constant at $t=0$; i.e., $A_2(0)=[A_2]_0$. The parameters λ_1 and λ_2 are closely related to the lifetimes of states 2 and 3, respectively, and the factors s_1 and s_2 represent the statistical weights.

If the rate coefficient of collisional activation k_{-3} is negligible, then λ_1 and λ_2 reduce to C_{11} and C_{22}, which correspond to the reciprocal of the effective lifetimes of states 2 and 3, respectively. Since s_2 appears to be very small, the time evolution of $A_2(t)$ predominantly follows a single exponential function. The weight of s_2 increases as the collisional activation rate increases.

For determining λ_1 and λ_2 parameters, a computer simulation to fit the time-resolved spectrum is a common, reliable method and has been employed frequently. Alternatively, if the collision mixing between the two states are weak, then the population in state 2 (or $n\,^2S$) can evolve in a form of single exponential function. The related effective lifetime may be easily determined. The following two situations correspond to experimental conditions for which there occurs only a weak collision coupling between these two states. First, in the initial period after excitation, while only very little population in state 3 has yet accumulated, the rate of collisional activation to the state 2 is negligible. Neglecting the collisional activation process in Eq. (3) simplifies the solution as follows:

$$[A_2(t)] \sim [A_2]_0 e^{-C_{11} t} \;. \tag{14}$$

Note that only in the early period can the decay curve of the state 2 be treated as a single exponential function, from which the effective lifetime, associated with collisions of K and H_2, may be derived without significant disturbance by the other K atomic states. Second, when the number density of the H_2 gas is small, i.e., $C_{11}C_{22} \gg C_{12}C_{21}$, the values of λ_1 and λ_2 reduce to k_1 and k_4, respectively. Substitution into Eq. (6) produces

$$[A_2(t)] = [A_2]_0 e^{-k_1 t} \;. \tag{15}$$

It becomes straightforward to determine the radiative lifetime of the state 2 in the absence of H_2.

According to the Stern-Volmer equation, a plot of the reciprocal of the effective lifetime of the state 2 against the H_2 pressure yields a slope that indicates the total cross section for deactivation and an intercept at zero H_2 pressure, which provides the information on the radiative lifetime of the state. The related equation is

$$\frac{1}{\tau}=\frac{1}{\tau_0}+\sigma v_{\text{K-H}_2}[\text{H}_2] \, , \tag{16}$$

where τ is the effective lifetime, τ_0 the natural radiative lifetime of the state 2, $v_{\text{K-H}_2}$ the Maxwellian averaged relative velocity for K-H_2 collision, σ the total cross section for deactivation, and $[H_2]$ the number density of H_2. The radiative lifetime and the total cross section for deactivation of the K($n\,^2D$) state, excited by two-photon absorption, can also be determined through the analogous procedure.

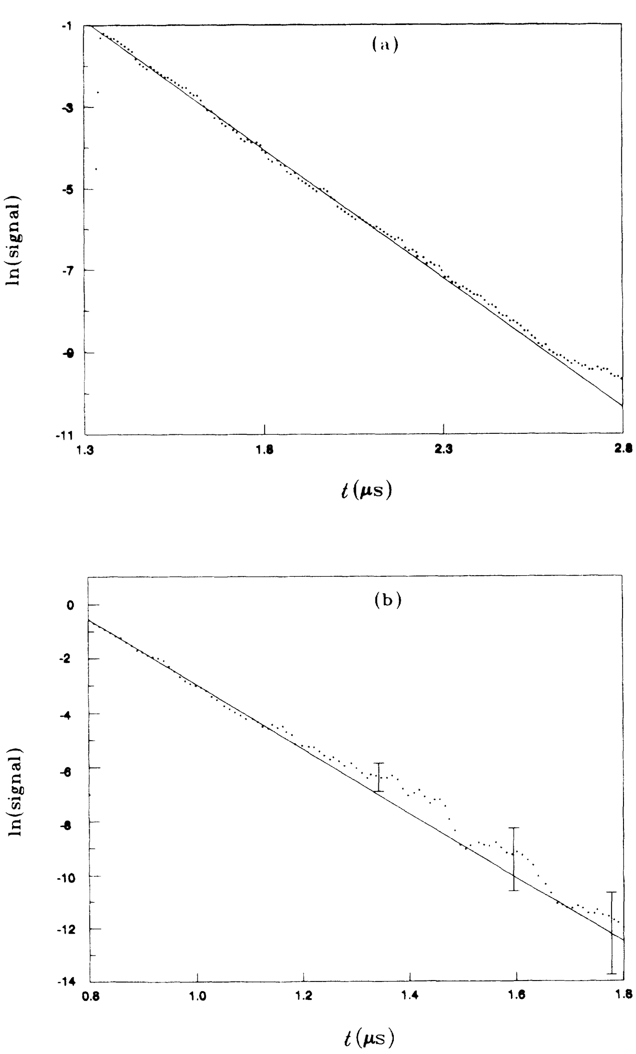

FIG. 2. Semilogarithmic plot for time-resolved fluoresence of the K atom in the $8\,^2S$–$4\,^2P$ transition. The effective lifetime determined from the early period of the decay curve yields (a) 159 ns at H_2 pressure of 44 mTorr, (b) 84 ns at H_2 pressure of 106 mTorr. Note that the oscillation in (b) is insignificant when the error bar is considered.

IV. RESULTS AND DISCUSSION

According to Eq. (14), we have determined the effective lifetimes of the K $n\,^2S$ states in the presence of H_2 by taking the portion within the early period with a slight correction from the long-time decay curve [16]. Figure 2 gives the example of the time-resolved spectrum for the K $8\,^2S$ state. The lifetime for the depopulation of the K $n\,^2D$ states can be treated analogously; Fig. 3 presents part of the results. Based on the Stern-Volmer equation given in Eq. (16), Figs. 4 and 5 show the resulting plots for the cases of K $n\,^2S$ ($n=8$–11) and $n\,^2D$ ($n=6$–8) states. The results for the radiative lifetimes and the total cross sections for deactivation by H_2 are listed in Table I.

The kinetic model has been successfully applied to the determination of the lifetimes for the K $7\,^2S$ and $5\,^2D$ states previously [12]. We have demonstrated that the H_2 collision-induced $7\,^2S$–$5\,^2D$ transition is the predominant channel for the depopulation process of the K $7\,^2S$ state [12]. In the near-resonant collision transfer from the $n\,^2S$ state, $(n-2)^2D$ is the nearest state and therefore the only one that should be considered in a three-level system.

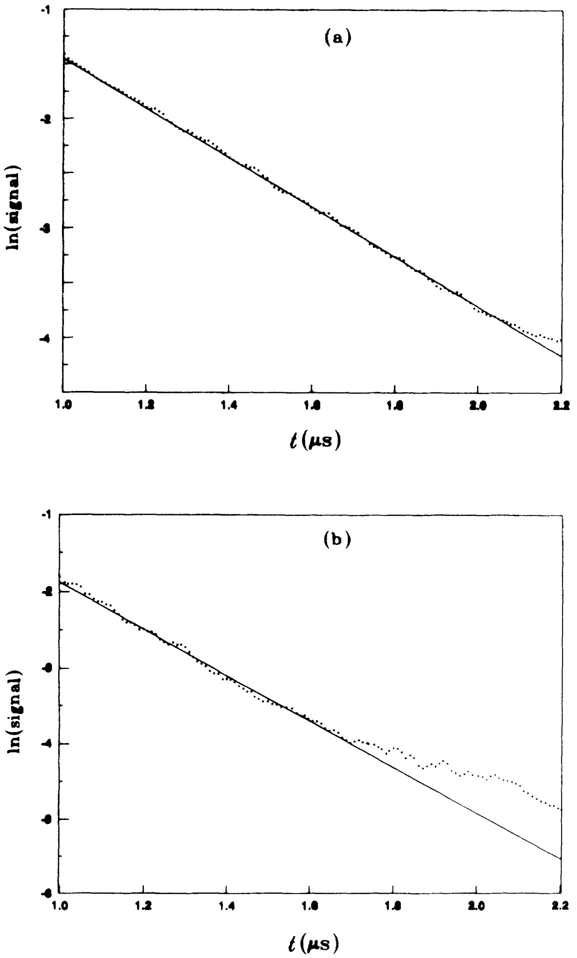

FIG. 3. Semilogarithmic plot for time-resolved fluorescence of K atom in the $6\,^2D$–$4\,^2P$ transition. The effective lifetime determined from the early period of the decay curve yields (a) 432 ns at H_2 pressure of 49 mTorr, (b) 306 ns at H_2 pressure of 122 mTorr.

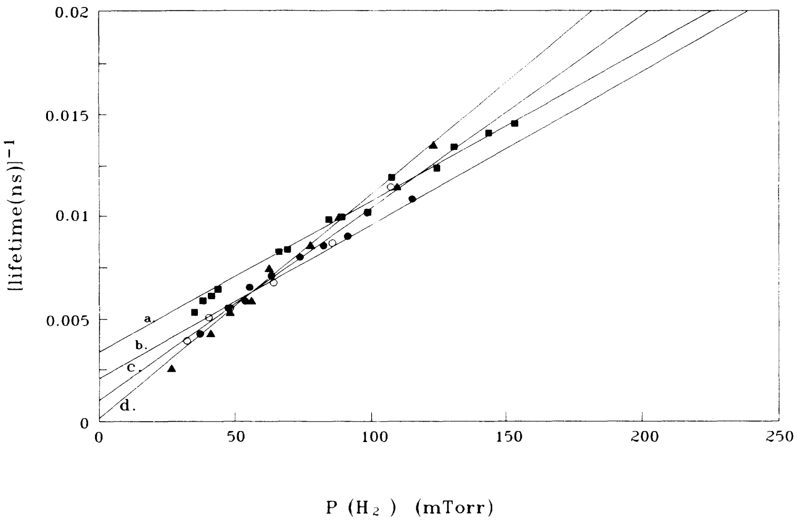

FIG. 4. Stern-Volmer plot [Eq. (16)] of the reciprocal of the effective lifetime for the K $n\,^2S$ ($n=8$–11) states as a function of the H_2 pressure. (a) $n=8$ (■); (b) $n=9$ (●); (c) $n=10$ (○); (d) $n=11$ (▲).

The criterion for a valid application of Eq. (14) relies on the condition of a weak collision coupling between the S and D states; i.e., the activation rate from the D state must be small. We may estimate this coefficient using the principle of detailed balance,

$$\frac{k_3}{k_{-3}}=\frac{g_3}{g_2}e^{\Delta E/k_B T}\,, \tag{17}$$

where g_2 and g_3 denote the statistical weight for the $n\,^2S$ and $(n-2)^2D$ states, respectively; ΔE is the energy difference between them, and k_B is the Boltzmann constant. The coefficient k_{-3} appears to be small due to a large factor of g_3. The ratio k_{-3}/k_3 involved in the case of $7\,^2S$–$5\,^2D$ transfer, for instance, is only about 0.153 [12]. For the high-lying $n\,^2D$ states, it has been found that the collisional orbital angular momentum mixes strongly with the $l>2$ states of the same n [8,10,17]. This fact leads to a much larger statistical weight for the state of D manifolds. In addition, the lifetimes of the D states have been measured to be much longer than those for the S states. That also leads to a significant difference between the parameters λ_1 and λ_2. Although the S-D state energy difference is small, the nature of long lifetime and collisional mixing, associated with the D state, does slow down the activation rate. Thus the collisional coupling between the D-S states is expected to be weak. This is confirmed by the fact that the radiative lifetimes we obtain in this work are consistent with both the results by computer simulation and those reported elsewhere [18–21].

As shown in Table I, it has been found that the cross sections for the $n\,^2S$ states increase with increasing principal quantum number n, while those for the $n\,^2D$ states are almost ten times smaller and their n dependence ap-

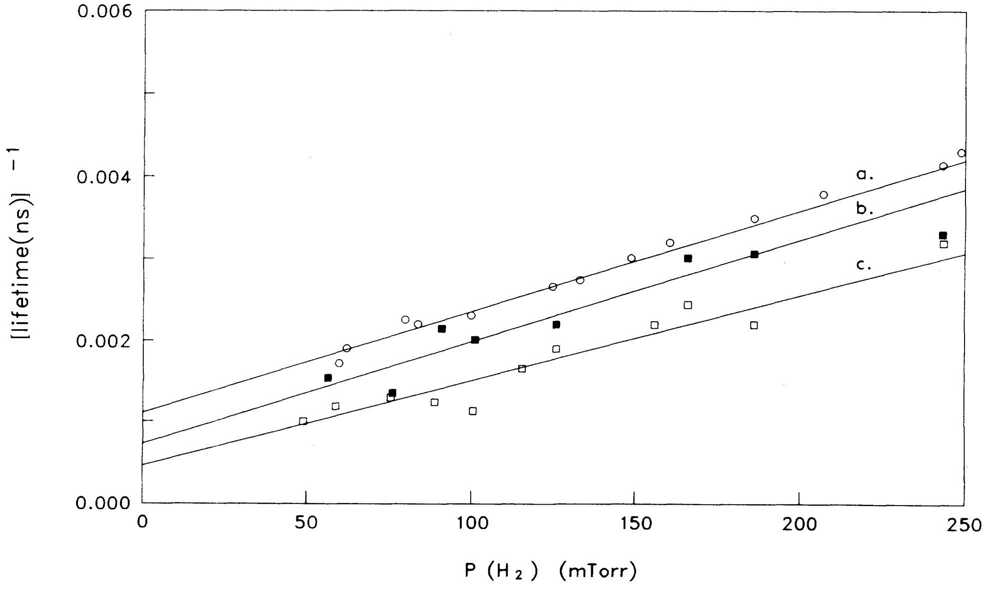

FIG. 5. Stern-Volmer plot [Eq. (16)] of the reciprocal of the effective lifetime for the K $n\,^2D$ ($n=6$–8) states as a function of the H_2 pressure. (a) $n=6$; (b) $n=7$; (c) $n=8$.

TABLE I. Radiative lifetimes and total cross sections for deactivation by H_2 of K $n\,^2S$ ($n=7$–11) and $n\,^2D$ ($n=5$–8) states.

	Lifetime (ns)					Cross section (Å^2)
		Others				
	This work	Ref. [17]	Ref. [18][b]	Ref. [19]	Ref. [20]	This work
7^2S	157(5)[a]	165(12)	157.8–152.8	160	160	150(2)[a]
8^2S	227(16)	260(14)	259.6–244.9	269.2	270	167(5)
9^2S	391(32)	441(18)	396.1–366.6	423.4	420	189(9)
10^2S	562(41)	600(13)	571.2–519.8	628.3	620	208(17)
11^2S	803(57)	910(12)	788.3–706.9	895.4	870	231(27)
5^2D	569(12)[a]	610(90)	749–692	720	710	39(4)[a]
6^2D	798(32)	890(60)	1087–943	1066	1050	26(4)
7^2D	1269(42)	1210(100)	1390–1169	1416	1500	28(3)
8^2D	1579(73)	1590(130)	1742–1440	1844	1910	20(2)

[a] See Ref. [12].

[b] Temperature range 355–600 K.

pears to decrease. Similar results have also been reported in the quenching processes by noble gas, N_2 and CO of the excited Na atom in the $n\,^2S$ and $n\,^2D$ states [8–10]. For the case of the $n\,^2S$ states, the ion core has a weak binding force for the outer-shell *ns* electron, and thus the effective size of these highly excited atoms and their subsequent collisional cross sections increase with increasing *n*. It can also be alternatively interpreted by the model of electron harpoon. Because the curve crossing region between the attractive ionic surface and the repulsive covalent surface moves towards a larger interparticle distance with increase of *n*, that leads to an increase of the deactivation cross section [22]. According to the harpoon model, the cross section can be expressed as

$$\sigma = f\pi r_c^2 \ , \tag{18}$$

where r_c is the ionic-covalent crossing radius, f denotes the fraction of covalent surfaces resulting from each excited atomic state that correlates with the ionic surface. For a C_{2v} symmetry of transition-state intermediate, $f=1$ for the $n\,^2S$ states and $f=0.4$ for the $n\,^2D$ states [11]. A smaller deactivation cross section found in the low-lying ^2D states can be understood qualitatively in terms of symmetry correlation. However, this simple picture cannot explain the n dependence of the cross sections observed for the $n\,^2D$ states.

Gallagher *et al.* have measured the collisional mixing cross sections of highly excited Na($n\,^2D$) with $l>2$ states using noble gases, N_2, and CO as collision partners [8,10,17]. They found that the cross sections are on the order of 1000 Å^2. The collisional mixing rate is so fast that the observed lifetime for $n\,^2D$ actually corresponds to the average lifetime of all the $l \geq 2$ states of the same n. In the following, we can use the same kinetic model as in the preceding section to interpret the phenomenon. In the reaction scheme 1–5, A_2 and A_3 are replaced by the $n\,^2D$ state and $l>2$ manifold, respectively, and are considered to be coupled very strongly, so that the states reach equilibrium rapidly. Therefore, we may assume that the value of k_3/k_{-3} equals the relative ratio of the corresponding statistical weights, g_3 and g_2, for the states 3 and 2, i.e.,

$$\frac{k_3}{k_{-3}} = \frac{g_3}{g_2} \ . \tag{19}$$

The rate coefficients $k_3[H_2]$ and $k_{-3}[H_2]$ should dominate over the other reaction channels. By applying the binomial expansion, λ_1 and λ_2 in Eq. (13) can be simplified to

$$\lambda_1 \sim (C_{11}+C_{22}) - \frac{(C_{11}C_{22}-C_{12}C_{21})}{(C_{11}+C_{22})} \ , \tag{20}$$

$$\lambda_2 \sim \frac{C_{11}C_{22}-C_{12}C_{21}}{C_{11}+C_{22}} \ . \tag{21}$$

The population of $A_2(t)$ evolves predominantly following the term $e^{-\lambda_2 t}$ because of $\lambda_1 \gg \lambda_2$. Substitution of Eqs. (9)–(12) and (19) into Eq. (21) produces

$$\lambda_2 \sim \frac{g_3(k_5[H_2]+k_4)+g_2(k_2[H_2]+k_1)}{g_2+g_3} \ , \tag{22}$$

where λ_2 is related to the effective lifetime of the $n\,^2D$ state. However, the result obtained in Eq. (22) corresponds to an average lifetime for all the $l \geq 2$ states of the same n, in agreement with the observation by Gallagher *et al.*

Since the collision-induced mixing of the orbital angular momentum is so rapid, the total cross section for deactivation measured for the $n\,^2D$ state is closely related to the manifold of $l \geq 2$ states of the same n. According to the harpoon model, the exit channel that removes the energy after a collision is through three or four potential curves at most. The effective quenching rate therefore depends on the competition between the manifold and the lower atomic states for the exit channels. As the quantum number n increases, the energy separation between different $l \geq 2$ states becomes smaller. That leads to more states with $l \geq 2$ involved in the mixing, and their mixing rate inside the manifold also becomes faster. Therefore, as suggested by Gallagher *et al.* [8–10] the more states are included in the manifold as n increases, the less effective the deactivation process becomes. This can qualitatively explain the n dependence of cross section for the $n\ ^2D$ states.

In summary, we have successfully used a kinetic model of rate equations to interpret the temporal behavior of the K $n\ ^2S$ and $n\ ^2D$ states in the presence of H_2. The cross sections for the $n\ ^2S$ states increase with increasing n, whereas the cross sections for the $(n-2)^2D$ states are about ten times smaller and their n dependence tends to decrease gradually.

ACKNOWLEDGMENT

This work was supported financially by the National Science Council of the Republic of China under the Contract No. 81-0417-M001-01.

---

*Author to whom correspondence should be addressed.

[1] D. Paillard, J. M. Mestdagh, J. Cuvellier, P. de Pujo, and J. Berlande, J. Chem. Phys. **87**, 2084 (1987).
[2] C. Desfrancois, J. P. Astruc, R. Barbe, and J. P. Schermann, J. Chem. Phys. **88**, 3037 (1988).
[3] J. P. Astruc, C. Desfrancois, R. Barbe, and J. P. Schermann, J. Chem. Phys. **88**, 106 (1988).
[4] J. Cuvellier, L. Petijean, J. M. Mestdagh, D. Paillard, P. de Pujo, and J. Berlande, J. Chem. Phys. **84**, 1451 (1986).
[5] C. Crepin, J. L. Picque, G. Rahmat, J. Verges, R. Vetter, F. X. Gadea, M. Pelissier, F. Spiegelmann, and J. P. Malrieu, Chem. Phys. Lett. **110**, 395 (1984).
[6] F. X. Gadea, J. M. Lhermite, G. Rahmat, and R. Vetter, Chem. Phys. Lett. **151**, 183 (1988).
[7] T. F. Gallagher, G. A. Ruff, and K. A. Safinya, Phys. Rev. A **22**, 843 (1980).
[8] T. F. Gallagher, S. A. Edelstein, and R. M. Hill, Phys. Rev. A **15**, 1945 (1977).
[9] T. F. Gallagher, R. E. Olson, W. E. Cooke, S. A. Edelstein, and R. M. Hill, Phys. Rev. A **16**, 441 (1977).
[10] L. M. Humphrey, T. F. Gallagher, W. E. Cooke, and S. A. Edelstein, Phys. Rev. A **18**, 1383 (1978).
[11] K. C. Lin and H. C. Chang, J. Chem. Phys. **90**, 6151 (1989).
[12] H. C. Chang, Y. L. Luo, and K. C. Lin, J. Chem. Phys. **94**, 3529 (1991).
[13] C. Fabre and S. Haroche, in *Rydberg States of Atoms and Molecules,* edited by R. F. Stebbing and F. B. Dunning (Cambridge University Press, Cambridge, 1983), p. 117.
[14] K. C. Lin and C. T. Huang, J. Chem. Phys. **91**, 5387 (1989).
[15] K. C. Wang, K. C. Lin, and W. T. Luh, J. Chem. Phys. **96**, 349 (1992).
[16] A. Corney, *Atomic and Laser Spectroscopy* (Oxford University, Oxford, 1977), pp. 142–177.
[17] T. F. Gallagher, S. A. Edelstein, and R. M. Hill, Phys. Rev. Lett. **35**, 644 (1975).
[18] C. E. Theodosiou, Phys. Rev. A **30**, 2881 (1984).
[19] A. Lindgaard and S. E. Nielsen, At. Data Nucl. Data Tables **19**, 533 (1977).
[20] P. F. Grudzev and V. I. Denisov, Opt. Spektrosk. **52**, 15 (1982) [Opt. Spectrosc. (USSR) **52**, 8 (1982)].
[21] T. F. Gallagher and W. E. Cooke, Phys. Rev. A **20**, 670 (1979).
[22] E. Bauer, E. R. Fisher, and R. F. Gilmore, J. Chem. Phys. **51**, 4173 (1969).